

Reversible Dysfunction of Wild-Type p53 following Homeodomain-Interacting Protein Kinase-2 Knockdown

Rosa Puca,¹ Lavinia Nardinocchi,¹ Hilah Gal,^{4,5} Gideon Rechavi,⁶ Ninette Amariglio,⁶ Eytan Domany,⁵ Daniel A. Notterman,⁷ Marco Scarsella,² Carlo Leonetti,² Ada Sacchi,¹ Giovanni Blandino,^{1,3} David Givol,⁴ and Gabriella D'Orazi^{1,8}

¹Molecular Oncogenesis Laboratory and ²Preclinical Experimental Laboratory, Regina Elena Cancer Institute; ³Rome Oncogenomic Center, Rome, Italy; Departments of ⁴Molecular Cell Biology and ⁵Physics of Complex Systems, Weizmann Institute of Science, Rehovot, Israel; ⁶Department of Pediatric Hemato-Oncology, Chaim Sheba Medical Center, Tel-Hashomer and Sackler School of Medicine, Tel-Aviv University, Tel-Aviv, Israel; ⁷Department of Molecular Biology, Princeton University, Princeton, New Jersey; and ⁸Department of Oncology and Neurosciences, University "G. D'Annunzio," Chieti, Italy

Abstract

About half of cancers sustain mutations in the *TP53* gene, whereas the other half maintain a wild-type p53 (wtp53) but may compromise the p53 response because of other alterations. Homeodomain-interacting protein kinase-2 (HIPK2) is a positive regulator of p53 oncosuppressor function. Here, we show, by microarray analysis, that wtp53 lost the target gene activation following stable knockdown of HIPK2 (HIPK2i) in colon cancer cell line. Our data show that the stable knockdown of HIPK2 led to wtp53 misfolding, as detected by p53 immunoprecipitation with conformation-specific antibodies, and that p53 protein misfolding impaired p53 DNA binding and transcription of target genes. We present evidence that zinc supplementation to HIPK2i cells increased p53 reactivity to conformation-sensitive PAb1620 (wild-type conformation) antibody and restored p53 sequence-specific DNA binding *in vivo* and transcription of target genes in response to Adriamycin treatment. Finally, combination of zinc and Adriamycin suppressed tumor growth *in vivo* and activated misfolded p53 that induced its target genes in nude mice tumor xenografts derived from HIPK2i cells. Bioinformatics analysis of microarray data from colon cancer patients showed significant association of poor survival with low HIPK2 expression only in tumors expressing wtp53. These results show a critical role of HIPK2 in maintaining the retranscription activity of wtp53 and further suggest that low expression of HIPK2 may impair the p53 function in tumors harboring wtp53. [Cancer Res 2008;68(10):3707–14]

Introduction

The human *p53* gene is mutated in ~50% of human cancers, and in cancers harboring wild-type p53 (wtp53), its activity may be compromised by other mechanisms, including deregulation of regulatory proteins (1, 2). Various types of stress activate p53 mostly at posttranslational level, resulting in protein stabilization and in conformational changes that increase the affinity of the protein for specific DNA sequences (3). This active form of p53

leads to the expression of numerous target genes involved in oncosuppressor functions (4).

At present, the sequence-specific transcriptional activity represents a clear link between wtp53 biochemical activities and wtp53-mediated biological functions. In this regard, it has been shown that p53 phosphorylation at Ser46 is a late event after DNA damage and is a necessary step for inducing apoptosis in response to severe DNA damage (5). Thus, the specific p53Ser46 phosphorylation is considered to be a sensor for DNA damage intensity that promotes changes in p53 affinity for different promoters with a shift from cell cycle arrest-related genes to apoptosis-related genes (5, 6). Thus, deletion of the transcriptional activation domain (TAD) 2 (residues 43–63) of p53 abolishes apoptosis and phosphorylation at both Ser46 and Thr55 enhances the binding to p53 of p62 and Tfb1, which play an important role in regulating p53 target gene activation (7).

We and others have shown that homeodomain-interacting protein kinase-2 (HIPK2) specifically phosphorylates p53 at Ser46, in response to severe DNA damage, regulating p53-induced apoptosis by enhancing the p53-mediated transcriptional activation of proapoptotic factors such as p53AIP1, PIG3, Bax, Noxa, and KILLER/DR5 (8–11). Thus, it has been shown that silencing of endogenous HIPK2 by RNA interference reduces both p53Ser46 phosphorylation and p53 apoptotic function in response to drug (10). Recently, HIPK2 mutations in the speckle retention signal domain have been found in leukemias (12). Those HIPK2 mutations affect HIPK2 localization and impair p53-mediated transcription. Therefore, further identification of mechanisms involving HIPK2-mediated p53 regulation may provide additional insights into the molecular etiology of the human cancers harboring wtp53.

Another important mechanism controlling p53 function is its conformational stability. The X-ray crystallography elucidated the DNA-binding domain structure of p53 and shows the importance of zinc atom in stabilizing this structure (13). Treatment of wtp53 with metal chelators *in vitro* results in removal of zinc and disruption of the tertiary structure, with loss of sequence-specific DNA binding to the canonical p53-binding site (14, 15). Conversely, addition of zinc allows p53 folding into wild-type conformation (16).

Here, we show the involvement of HIPK2 in maintaining wtp53 native conformation for a proper transcription activity after DNA damage. We found that chronic depletion of HIPK2 function by stable interference with pSUPER vector (HIPK2i) resulted in complete abolishment of p53 transcription activity in response to chemotherapeutic drug Adriamycin in colon cancer cell line. In this system, p53 acquired a misfolded conformation leading to loss of

Note: Supplementary data for this article are available at Cancer Research Online (<http://cancerres.aacrjournals.org/>).

R. Puca and L. Nardinocchi contributed equally to this work.

Requests for reprints: Gabriella D'Orazi, Molecular Oncogenesis Laboratory, Regina Elena Cancer Institute, Via delle Messi d'Oro 156, 00158 Rome, Italy. Phone: 39-06-52662542; Fax: 39-06-52662505; E-mail: gdorazi@unich.it.

©2008 American Association for Cancer Research.

doi:10.1158/0008-5472.CAN-07-6776

the wtp53 transcription activity. Interestingly, zinc supplementation to HIPK2i cells induced regain of the wtp53 native conformation and transcription activity *in vitro*. In agreement with these data, treatment of mice carrying HIPK2i tumors with a combination of zinc and Adriamycin enhanced growth suppression of such tumors with regaining of wtp53 transcription activity *in vivo*. Altogether, these data indicate that HIPK2 can regulate wtp53 functions also through conformational variables and this conformational switch is reversible. The implication of these results to treatment of cancer with wtp53 and low expression of HIPK2 is discussed.

Materials and Methods

Cells and reagents. The engineered C-RKO and HIPK2i colon cancer cells were generated by stable transduction of pSUPER vectors carrying HIPK2 or aspecific RNA interfering sequences (10) and selected as polyclonal populations; the RKO-p53i cell line was a kind gift from S. Soddu (Regina Elena Cancer Institute, Rome, Italy). Cells were maintained in RPMI 1640 (Life Technologies-Invitrogen) supplemented with 10% fetal bovine serum, antibiotics, 2.5 $\mu\text{mol/L}$ HEPES, and glutamine. For treatments, Adriamycin and ZnCl_2 were added to the culture medium to a final concentration of 2 $\mu\text{g/mL}$ and 100 $\mu\text{mol/L}$, respectively, for the indicated period.

Viability and terminal deoxynucleotidyl transferase-mediated dUTP nick end labeling assays. Exponentially proliferating cells were exposed to Adriamycin (2 $\mu\text{g/mL}$) for different time points. Both floating and adherent cells were collected and counted in hemocytometer after addition of trypan blue. The percentage of dead cells (i.e., blue/total cells) was determined by scoring 100 cells per chamber for three times. At least three independent experiments were performed and cell numbers were determined in duplicate.

For terminal deoxynucleotidyl transferase-mediated dUTP nick end labeling (TUNEL) assay, both floating and adherent cells were spun onto slides by cytocentrifugation. After fixing in 4% paraformaldehyde, cells were permeabilized in 0.1% Triton X-100 and then incubated with fluorescein-conjugated dUTP terminal deoxynucleotide transferase mixture for TUNEL reaction according to the manufacturer's instructions (Roche). Cells were counterstained with Hoechst before analysis with a fluorescent microscope. At least 400 cells were counted in each plate in duplicate. At least three independent experiments were performed. Cell numbers were determined in duplicate.

Hybridization and analysis of gene expression by microarrays. C-RKO, HIPK2i, and p53i cells were treated with Adriamycin (2 $\mu\text{g/mL}$) and harvested after 8 and 16 h of treatment. Total RNA was extracted and used to synthesize biotin-labeled cRNA (4) and hybridized to separate Affymetrix Hu133A oligonucleotide arrays containing 22,215 probe sets (Affymetrix). Every sample was performed in triplicate. Gene expression values <20 were adjusted to 20 to eliminate noise from the data, and subsequently, all values were \log_2 transformed. Expression level ratios for each group were determined at time points 8 and 16 h, with respect to time 0 of the particular group. Only genes with expression ratios above >2 (or <0.5) in one or both time points of a particular treatment group were selected. The modulated gene lists were presented in Venn diagrams that compared the common and specific genes in each treatment group. We applied the sorting points into neighborhoods (SPIN) algorithm on the up-regulated genes. SPIN is an unsupervised method for analysis, organization, and visualization of the data (17).

RNA extraction and reverse transcription-PCR. Cells and tumors were harvested in Trizol Reagent (Invitrogen) and total RNA was isolated following the manufacturer's instructions. The first-strand cDNA was synthesized according to the manufacturer's instructions (Moloney murine leukemia virus reverse transcriptase kit, Applied Biosystems). Semiquantitative reverse-transcribed PCR was carried out by using HotMaster Taq (Eppendorf) using 2 μL cDNA reaction and gene-specific oligonucleotides under conditions of linear amplification. PCR was performed in duplicate in two different sets of cDNA. PCR products were run on a 2% agarose gel

and visualized with ethidium bromide. The housekeeping aldolase A and glyceraldehyde-3-phosphate dehydrogenase (GAPDH) mRNA, used as internal standard, were amplified from the same cDNA reaction mixture.

Chromatin immunoprecipitation assay. Chromatin immunoprecipitation (ChIP) analysis was carried out essentially as described (18). Briefly, cells were cross-linked with 1% formaldehyde for 10 min at room temperature and formaldehyde was then inactivated by the addition of 125 mmol/L glycine. Chromatin extracts containing DNA fragments with an average size of 500 bp were incubated overnight at 4°C with milk shaking using polyclonal anti-p53 antibody (FL393; Santa Cruz Biotechnology). Before use, protein G (Pierce) was blocked with 1 $\mu\text{g}/\mu\text{L}$ sheared herring sperm DNA and 1 $\mu\text{g}/\mu\text{L}$ bovine serum albumin for 3 h at 4°C and then incubated with chromatin and antibody for 2 h at 4°C. PCR was performed with HotMaster Taq using 2 μL of immunoprecipitated DNA and promoter-specific primers spanning p53-binding sites. Immunoprecipitation with nonspecific immunoglobulins (IgG; Santa Cruz Biotechnology) was performed as negative controls. PCR products were run on a 2% agarose gel and visualized with ethidium bromide.

Western blotting and p53 immunoprecipitation. Total cell extracts were prepared by incubation in lysis buffer [50 mmol/L Tris-HCl (pH 7.5), 300 mmol/L NaCl, 5 mmol/L EDTA, 150 mmol/L KCl, 1 mmol/L DTT, 1% NP40] and a mix of protease inhibitors (Sigma) and resolved by SDS-polyacrylamide gel electrophoresis. Proteins were transferred to a polyvinylidene difluoride (PVDF) membrane (Millipore) and incubated with the primary antibodies followed by an anti-IgG-horseradish peroxidase antibody (Bio-Rad). Specific proteins were detected by enhanced chemiluminescence (ECL; Amersham). Immunoblotting was performed with rabbit polyclonal anti-caspase-3, mouse monoclonal anti-poly(ADP-ribose) polymerase (PARP; all from BD PharMingen), rabbit polyclonal anti-p53Ser46 (Cell Signaling), rabbit polyclonal anti-p53 (FL393), and rabbit polyclonal anti-p21 (Santa Cruz Biotechnology) antibodies used in accordance with the manufacturer's instruction and revealed by ECL kit (Amersham). Mouse monoclonal anti-tubulin (Immunological Sciences) was used as protein loading control.

For p53 immunoprecipitation, cells were lysed in immunoprecipitation buffer [10 mmol/L Tris (pH 7.6), 140 mmol/L NaCl, 0.5% NP40, protease inhibitors] for 20 min on ice and cleared by centrifugation. Precleared supernatants (200 μg) were immunoprecipitated overnight at 4°C with the conformation-specific monoclonal antibodies PAb1620 (wild-type specific) and PAb240 (mutant specific; Calbiochem) preadsorbed to protein G-agarose (Pierce). Immunocomplexes were collected by centrifugation, separated by 9% SDS-PAGE, and blotted onto PVDF membrane. Immunoblotting was performed with rabbit polyclonal anti-p53 (FL393) antibody and revealed by ECL kit.

Transactivation assay. Cells were transiently transfected with the luciferase reporter gene driven by the p53-dependent synthetic PG13-luc (kindly provided by M. Oren, Weizmann Institute, Rehovot, Israel), natural Noxa-luc (kindly provided by T. Taniguchi, University of Tokyo, Tokyo, Japan), and AIP1-luc (kindly provided by H. Arakawa, National Cancer Center, Tokyo, Japan) promoters using Lipofectamine Plus (Invitrogen) method according to the manufacturer's instructions. Twenty-four hours after transfection, cells were treated with Adriamycin (2 $\mu\text{g/mL}$) for additional 12 h. Transfection efficiency was normalized with the use of a cotransfected β -galactosidase plasmid. Luciferase activity was assayed on whole-cell extract and the luciferase values were normalized to β -galactosidase activity and protein content.

Tumorigenicity in nude mice. Six-week-old CD-1 nude (*nu/nu*) mice (Charles River Laboratories) were used for *in vivo* studies. For tumor treatments, 3×10^6 viable RKO-HIPK2i cells were implanted i.m. on the flank of each mouse, allowing the tumors to grow to 400 mm^3 weight (approximately 5–7 d from injection). Mice were then randomized in four groups (six to eight mice per group) and treated with Adriamycin (10 mg/kg body weight), ZnCl_2 (10 mg zinc/kg body weight), combination of Adriamycin plus ZnCl_2 , or PBS. Adriamycin was injected once at day 7, i.p., whereas ZnCl_2 was administered once daily by oral administration, starting from day 7, over the course of 2 wk. Tumor dimensions were measured every other day and their volumes were calculated from caliper

measurements of two orthogonal diameters (x and y , larger and smaller diameters, respectively) by using the formula volume = $xy^2/2$, as previously described (19). The antitumor effect of the combination treatment zinc + Adriamycin was evaluated by comparing the relative tumor size with tumors treated with Adriamycin only or zinc only. The experiment was repeated twice with similar results. All mouse procedures were carried out in accordance with institutional standard guidelines.

Statistical analyses. All experiments unless indicated were performed at least thrice. All experimental results were expressed as the arithmetic mean and SD of measurements was shown. Student's t test was used for statistical significance of the differences between treatment groups in tumor growth. Statistical analysis was performed using ANOVA at 5% ($P < 0.05$) or 1% ($P < 0.01$).

Survival plots were analyzed using the Kaplan-Meier method; survival of colon cancer patients with high (top tertile) and low (bottom tertile) expression levels of HIPK2 (obtained from microarray gene expression data) was compared separately for patients with wtp53 and mutant p53 (mutp53).

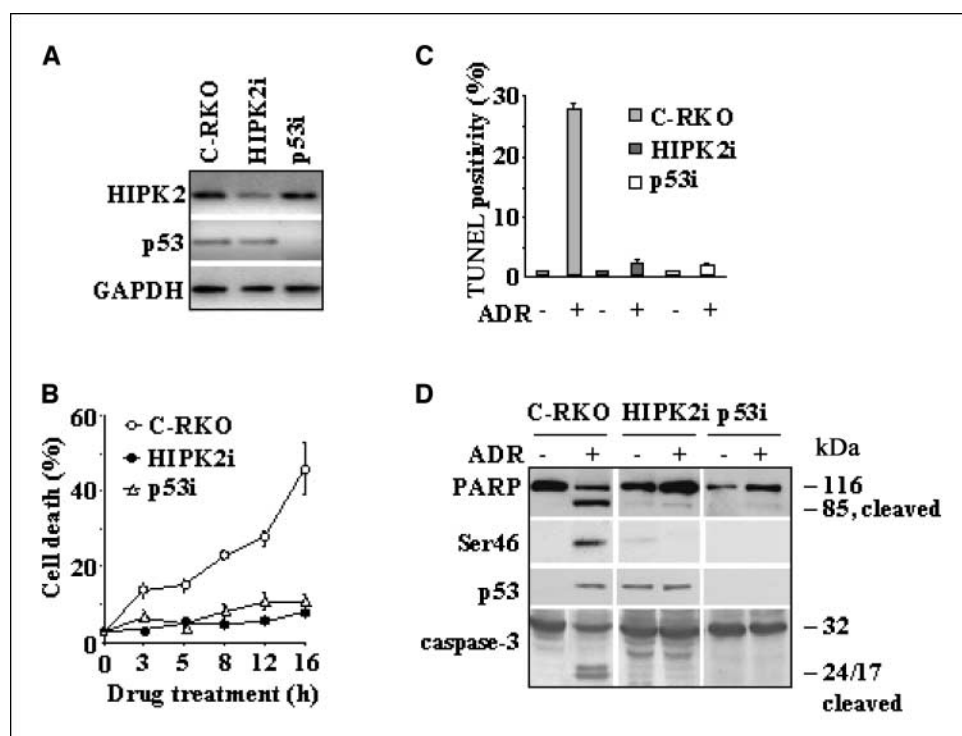
Results

Knockdown of either HIPK2 or p53 inhibits Adriamycin-induced apoptosis. To investigate the role of HIPK2 in p53 regulation, we compared RKO colon cancer cell line depleted of either the endogenous HIPK2 or p53 by stable transfection with pSUPER vectors carrying HIPK2, p53, or aspecific RNA interfering sequences. We first analyzed the expression of HIPK2 and p53 on small interfering RNA (siRNA) interference. As shown in Fig. 1A, HIPK2 and p53 expression was decreased in, respectively, RKO-HIPK2-interfered (HIPK2i) and RKO-p53-interfered (p53i) cells compared with that of control vector-transfected cells (C-RKO). To evaluate the biological consequences of either HIPK2 or p53 depletion, we verified the apoptotic response to chemotherapeutic treatment because results of our previous studies indicate that HIPK2 regulates p53Ser46-induced apoptosis in response to

severe DNA damage (8, 10). Here, we used the chemotherapeutic drug Adriamycin that has been shown to induce Ser46 phosphorylation and apoptosis (5). As shown by viability (Fig. 1B) and TUNEL (Fig. 1C) assays, HIPK2- and p53-depleted cells were both resistant to Adriamycin-induced cell death compared with the control C-RKO cells. In fact, we found that only C-RKO cells expressed PARP and caspase-3 cleavages compared with HIPK2- and p53-depleted cells (Fig. 1D). In agreement, C-RKO cells showed p53Ser46 phosphorylation that was inhibited in HIPK2i cells despite good expression of p53, whereas p53i cells showed absence of p53 (Fig. 1D). Altogether, these results indicate that although p53 accumulated in HIPK2 knockdown cells, its function was impaired.

Stable knockdown of HIPK2 inhibits p53 DNA-binding and transcription activity. To gain further insight into the alteration of p53 pathway, we compared gene expression patterns of C-RKO, HIPK2i, and p53i cells, treated with apoptotic dose of Adriamycin, by DNA microarray analyses. Expression ratios were determined for each group at time points 8 and 16 h after Adriamycin treatment, with respect to the time 0 h of each cell line. Only those genes that showed >2-fold induction or repression in one or both time points of a particular treatment group were considered and the genes that were modulated in the two time points were compared by the Venn diagram (Fig. 2A). The modulated genes in C-RKO cells on Adriamycin treatment identified 1,904 up-regulated and 2,791 down-regulated genes in at least one time point and among them were the known p53 targets (compared with Supplementary Table S2 in ref. 20; Supplementary Table S1). These p53 target genes were not modulated in HIPK2i cells, whereas some of them were still induced in p53i cells, including *CCNG2/Cyclin G2*, *ATF3*, and *CDKN1A/p21* (Supplementary Table S1), suggesting that the residual p53 in p53i cells retained the ability of activating some genes probably because of the higher affinity to their promoters.

Figure 1. Both HIPK2- and p53-depleted cell lines are resistant to Adriamycin-induced apoptosis. **A**, RT-PCR analysis of endogenous HIPK2 and p53, in RKO cells, depleted of either the endogenous HIPK2 or p53 by stable transfection with pSUPER vectors carrying HIPK2 (*HIPK2i*), p53 (*p53i*), or aspecific (*C-RKO*) RNA interfering sequences. The mRNA levels were normalized to GAPDH expression. **B**, the three cell lines as in **A** were treated with 2 μ g/mL Adriamycin (*ADR*) for the indicated period and the percentage of dead cells was scored by trypan blue staining. **Points**, mean of three independent experiments; **bars**, SD. **C**, the three cell lines were treated with Adriamycin for 24 h and analyzed by TUNEL assay. Quantitation of TUNEL-positive/apoptotic cells was performed with respect to total nuclei stained with Hoechst. **Columns**, mean of three independent experiments for each cell line; **bars**, SD. **D**, the three cell lines were treated with Adriamycin for 24 h. The expression of Ser46, p53, caspase-3, and PARP cleavage was determined by Western blotting with whole-cell lysates. The representative bands from at least two independent experiments are shown.



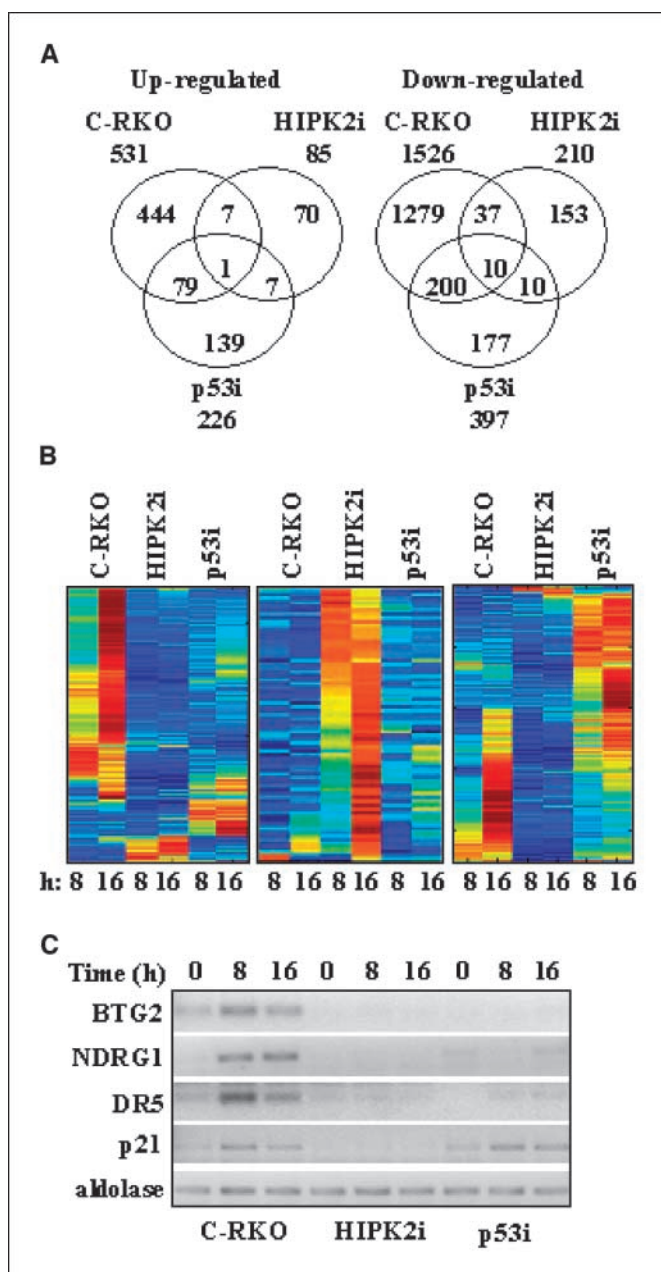


Figure 2. DNA microarray analyses of the C-RKO, HIPK2i, and p53i cell lines treated with Adriamycin for 8 and 16 h. *A*, Venn diagram comparison of the common and specific modulated genes in the three cell lines. Only genes that were modulated >2-fold or <2-fold at the two time points (see Materials and Methods) are shown. *B*, expression matrix of the modulated genes in the three cell lines after sorting using the SPIN algorithm. *Left*, matrix of the 747 genes up-regulated in all cell lines (see *A*); *middle*, matrix of the 85 genes specifically up-regulated in HIPK2i cells; *right*, matrix of the 226 genes specifically up-regulated in p53i cells. *C*, DNA microarray data validation by semiquantitative RT-PCR. Total mRNAs were reverse transcribed from C-RKO, HIPK2i, and p53i cells treated with Adriamycin (0, 8, and 16 h) for the PCR analyses of the indicated p53 target genes. The mRNA levels were normalized to aldolase expressions.

The SPIN algorithm (17) was used to order the expressed genes of the combined genes up-regulated >2-fold in both time points, in all three cell lines, as they appear in the Venn diagram (Fig. 2A), yielding 747 genes. This expression matrix confirmed that there was almost no overlap between up-regulated genes in C-RKO and

the interfered cells. The modulated genes in C-RKO were absent in HIPK2i and only very few of them were present in p53i cells (Fig. 2B, left). Analysis of the 85 genes up-regulated in HIPK2i showed that they were not induced in C-RKO nor in p53i cells (Fig. 2B, middle). Similarly, analysis of the 226 genes up-regulated in p53i cells showed that they were not induced in HIPK2i; however, few of them were induced in C-RKO cells (Fig. 2B, right). The microarray data were validated by reverse transcription-PCR (RT-PCR) analyses on a pool of activated genes (e.g., *BTG2*, *NDRG1*, *DR5*, and *p21*), with an aliquot of the RNA used in the DNA chip analyses (Fig. 2C). Similar results were obtained with a second set of cDNA (data not shown). The results showed that the p53 target genes induced in C-RKO cells were completely inhibited by HIPK2 depletion and in a lesser extent by p53 depletion. These data suggest that, despite siRNA, the p53 retained in p53i cells could still be able to activate its target genes (e.g., *p21*), whereas the transactivation activity of p53 in HIPK2i cells was completely impaired.

To further evaluate this hypothesis, we performed luciferase assay by transfecting a plasmid containing 13 copies of the p53-binding consensus sequence upstream of a luciferase reporter gene. As shown in Fig. 3A, the PG13-luc reporter activity was induced by Adriamycin treatment in C-RKO cells, whereas it was significantly impaired in HIPK2 knockdown cells, suggesting a lack of p53 protein transcription activity. To confirm this hypothesis, two natural promoters were analyzed. As shown in Fig. 3B, the Noxa-luc and AIP1-luc promoter activities were severely impaired in HIPK2i cells. To further understand the molecular mechanism by which HIPK2 knockdown inhibits p53 transactivation activity, we checked the binding of p53 to its target DNA sequences. ChIP analyses showed that the p53 binding to the target gene promoters (e.g., *BTG2*, *NDRG1*, and *DR5*) was enhanced in response to Adriamycin treatment in C-RKO cells (Fig. 3C, top), whereas it was hampered in HIPK2i cells (Fig. 3C, bottom). Overall, these data suggest that, when HIPK2 is depleted, the p53 protein is impaired in its DNA-binding and transcription activity.

Reversible misfolding of p53 protein in HIPK2i cells. p53 may lose its transcription activity either because of a mutation or because of conformational changes that reduce the affinity of the protein for specific DNA sequences. High p53 content, such as that is present in HIPK2i cells (Fig. 1D), and impaired p53 transcriptional activity, such as that seen in the above results, are a common feature of many solid tumors carrying out mutations in *p53* gene (21); therefore, we evaluated this hypothesis. Direct cDNA sequencing revealed the wild-type sequence of the endogenous p53 in HIPK2i cells (data not shown). High content and impaired p53 transcriptional activity is also the result of a change in the tertiary structure of p53 (15). Hence, the conformation of p53 was studied by immunoprecipitation technique using two conformation-specific antibodies, PAb1620 and PAb240, which identify folded ("wild-type") and unfolded ("mutant like") p53 structure, respectively (22, 23). As expected, C-RKO cells expressed mainly wtp53 as shown by the reactivity with PAb1620 (Fig. 4A). In HIPK2i cells, although the PAb1620-positive phenotype was present, an unfolded p53 isoform appeared, as identified by reactivity to PAb240 (Fig. 4A) that might be compatible with the loss of DNA-binding activity seen in Fig. 3. To determine whether this conformation status of p53 was reversible, the HIPK2i cells were treated with $ZnCl_2$ (16). As shown in Fig. 4B, zinc supplementation to Adriamycin treatment increased the folded PAb1620-reactive conformer, supporting the hypothesis that zinc plays a

role in the control of conformation of the misfolded p53 and that HIPK2 is involved in this regulation.

To evaluate the activation of wtp53-responsive genes after zinc supplementation, the *in vivo* promoter binding was analyzed by using ChIP. HIPK2i cells were treated with Adriamycin in the presence or absence of zinc and p53 was immunoprecipitated with polyclonal anti-p53 antibody (FL393). The amount of coprecipitated p53-binding element in target promoters was determined by RT-PCR. The results showed strong enrichment of p53 binding to its wild-type target promoters in response to Adriamycin only after zinc supplementation (Fig. 5A). The increase of p53 DNA binding in HIPK2i cells, treated with Adriamycin and zinc, was consistent with the level of induction of mRNAs of p53 target genes that were comparable with the wtp53-dependent gene expression in C-RKO cells treated with Adriamycin (Fig. 5B). This finding was also consistent with the increased p53 reactivity to PAb1620 seen in Fig. 4B. Finally, Western blot analysis showed induction of p21 expression by zinc treatment, suggesting restoration of misfolded p53 transcription function in HIPK2i cells (Fig. 5C). Therefore, zinc supplementation could reverse the misfolding of p53 and restore the sequence-specific DNA binding *in vivo* and the target gene transcription.

Activation of misfolded p53 in tumor xenografts. To test whether zinc activates misfolded p53 also *in vivo*, we generated

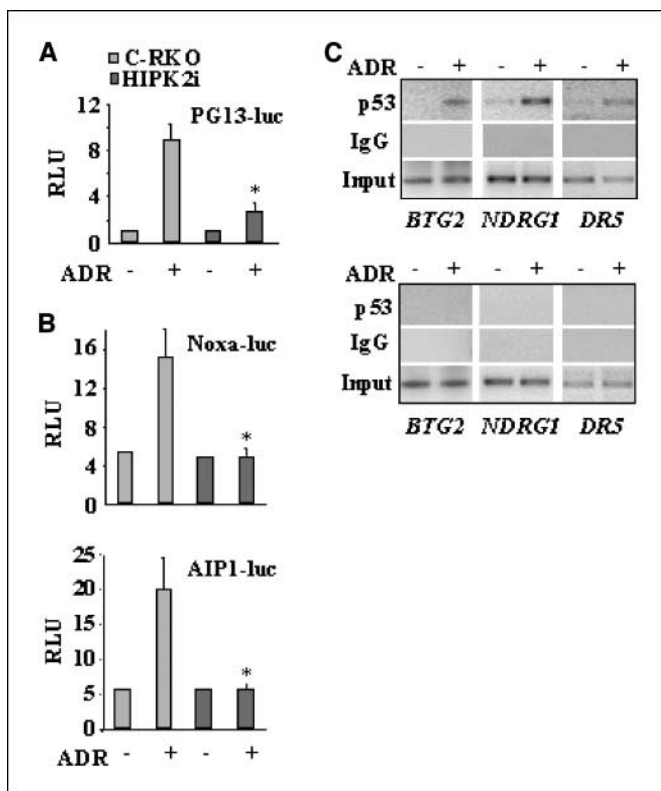


Figure 3. The p53 recruitment on gene promoters and its transcription activity is impaired by HIPK2i knockdown. Relative luciferase activity (RLU) of reporter constructs PG13-luc (A) and Noxa-luc and AIP1-luc (B) transfected in C-RKO and HIPK2i cells in the presence or absence of Adriamycin, showing significant impairment of p53-dependent transcription by HIPK2i knockdown compared with C-RKO cells. Columns, mean of three independent experiments performed in duplicate; bars, SD. *, $P < 0.01$. C, ChIP analyses performed with p53 antibody on C-RKO (top) and HIPK2i (bottom) cells treated with 2 μ g/mL Adriamycin for 16 h. Nonspecific IgG was used as control.

tumor xenografts in athymic nude mice by injecting HIPK2i cells. Cells were implanted into nude mice by i.m. injection and allowed to develop into ~ 400 mm³ tumor nodules at the injection sites. The mice were then treated with Adriamycin and ZnCl₂ separately or in combination (see Materials and Methods). Mice treated with zinc alone over the course of 2 weeks displayed tumor volume that increased in size in a comparable manner with those treated with vehicle PBS, reaching a volume of ~ 4 cm³ by day 21 (Fig. 6A). Mice treated with Adriamycin displayed an average tumor volume above 3 cm³ by day 21 that was not statistically significant compared with vehicle PBS- or zinc-treated mice ($P = 0.177$). Interestingly, mice treated with combination of zinc and Adriamycin showed a statistically significant reduction of tumor growth that remained < 2 cm³ by day 21 (Adriamycin + zinc versus Adriamycin: $P = 0.0121$; Adriamycin + zinc versus zinc: $P = 0.0002$; Fig. 6A). Tumors were harvested by day 18 and p53 target gene expression was determined by RT-PCR. The results showed that p53 target genes (e.g., *NDRG1* and *PIG3*) were induced by zinc supplementation to Adriamycin treatment compared with Adriamycin-injected tumors (Fig. 6B). These results suggest that zinc was able to reactivate the endogenous misfolded p53 in tumors *in vivo*.

Microarray analysis of HIPK2 expression on colon cancers. Our results may be relevant to the effect of wtp53, retained in $\sim 50\%$ of cancers, suggesting that for such tumors low levels of HIPK2 may be indicative of bad outcome. This hypothesis was addressed by analyzing expression microarray data on > 300 samples from colon cancer patients with known clinical records and p53 mutation status (known for a subset of the patients; ref. 24). We used carcinoma and clean metastasis samples and looked for association between HIPK2 expression and survival using the Kaplan-Meier procedure. From 60 wtp53 tumors, we extracted the high and low tertiles of HIPK2 expression levels ($n = 20$ patients in each group; ratio of average HIPK2 expression levels = 2.05). From 105 mutp53 tumors, we compared two groups of $n = 35$ in the high and low tertiles of expression (expression ratio = 2.02). The results showed that low expression of HIPK2 was associated with poor outcome in patients bearing tumors with wtp53 (Fig. 6C) but not in those with mutp53 (Fig. 6D). These results strengthen the role of HIPK2 in p53 regulation and highlight the possibility that combination treatment using chemotherapy and zinc may inhibit tumor growth, particularly in cancers with known wtp53 and low expression of HIPK2.

Discussion

The prevention and progression of human cancer development depend on the integrity of a complex network of defense mechanisms that help cells to respond to DNA damage and oncogenic stimuli. A key player in this network is p53 oncosuppressor, a DNA sequence-specific transcription factor (25). We have previously shown that HIPK2 regulates p53 oncosuppressor activity through Ser46 phosphorylation and induction of apoptotic target genes. Here, we have found that stable interference of HIPK2 function completely abolished p53 transcription activity in response to DNA damage, and investigated the mechanisms that may have led to loss of p53 function. We found that knockdown of HIPK2 resulted in misfolding of p53 that acquired a mutant-like conformation, concomitant with the loss of its wild-type transcription activity in response to Adriamycin. We showed regain of the wtp53 conformation and wild-type transcription

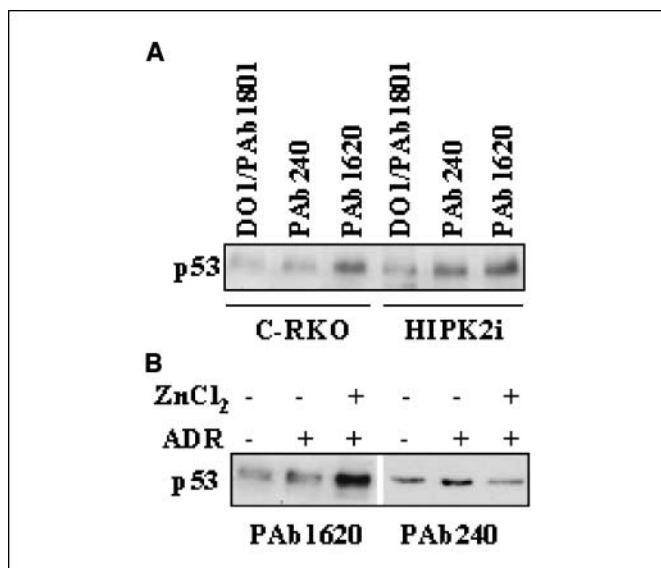


Figure 4. Immunoprecipitation of endogenous p53 with conformation-specific antibodies. *A*, C-RKO and HIPK2i total cell extracts were immunoprecipitated with conformation-specific antibodies PAb1620 (for wild-type, folded conformation) and PAb240 (for "mutant," unfolded conformation) and a mix of DO1 and PAb1801 (for both conformers). Immunoprecipitated total cell extracts were analyzed by Western blot with the FL393 polyclonal anti-p53 antibody. *B*, HIPK2i cells were treated with ZnCl₂ and Adriamycin and total cell extracts were immunoprecipitated as in *A*. The representative bands from at least two independent experiments are shown.

activity by zinc supplementation to Adriamycin treatment *in vitro*. Additionally, the treatment of transplanted human tumors, derived from HIPK2i cells, by the combination of zinc and Adriamycin inhibited synergistically tumor growth significantly better than Adriamycin alone, with regain of p53 transcription activity *in vivo*.

The p53 is an intrinsically unstable protein belonging to the group of intrinsically disordered proteins and this property is particularly located to the NH₂-terminal region encompassing Ser46 (26, 27). Therefore, p53 misfolding in our system could be due in part to the lack of Ser46 phosphorylation, which is in the TAD domain. Previous experiments showed that this NH₂-terminal region, outside of the DNA-binding domain (DBD), can affect the DBD function because antibodies to this region, particularly PAb1801 that recognizes the epitope encompassed by residues 46 to 55, confer on inactive mutp53 the regain of specific target DNA binding by the DBD (28).

The p53 structure includes one zinc atom as an important cofactor for DNA-binding activity *in vitro* (14) and *in vivo*, as some p53 mutations (e.g., C242S, H179R, C176F, and R175H) that perturb the zinc-binding site in p53 result in the loss of DNA binding (29). It has been proposed that metallothioneins might act as regulators of p53 folding and activity (16). Metallothionein is a class of cysteine-rich, metal-binding, antioxidant proteins that control the intracellular distribution of zinc and serve as a scavenger of reactive oxygen species (30). Metallothioneins also act as a potent chelator in removing zinc from p53 *in vitro* and may modulate p53 transcriptional activity (16). In addition, studies on the zinc-dependent folding of p53 DBD suggest that DBD must fold in an environment where free Zn²⁺ concentration is carefully regulated by cellular metalloproteins, although the concentration of free zinc in the cell is actually not known (31).

Interestingly, our microarray results showed stronger induction of metallothioneins in HIPK2i cells compared with C-RKO and p53i cells, in response to ADR treatment (data not shown). The finding that zinc supplementation reverted p53 dysfunction in our system strongly supports the hypothesis that p53 misfolding may be connected to zinc abstraction, and therefore, the measurement of intracellular levels of zinc in the presence and/or absence of HIPK2 would be of great interest in future studies. Several studies have shown an increased expression of metallothioneins in various human tumors (e.g., see ref. 32); therefore, additional studies are needed to address the differential metallothionein expression in tumors with down-regulated HIPK2. The functional importance of HIPK2 is evident by its numerous interacting proteins (e.g., transcriptional regulators and chromatin modifiers) and downstream phosphorylation targets, including p53 (reviewed in ref. 33). Therefore, masking or unmasking of p53 epitopes by additional interacting proteins regulated by HIPK2 may also be impaired following chronic HIPK2 depletion leading to p53 inactivations.

Altogether, the findings described in this article might account for the progression of tumors with impaired wtp53 in low HIPK2 background. It is noteworthy that an analysis of colon cancer patients

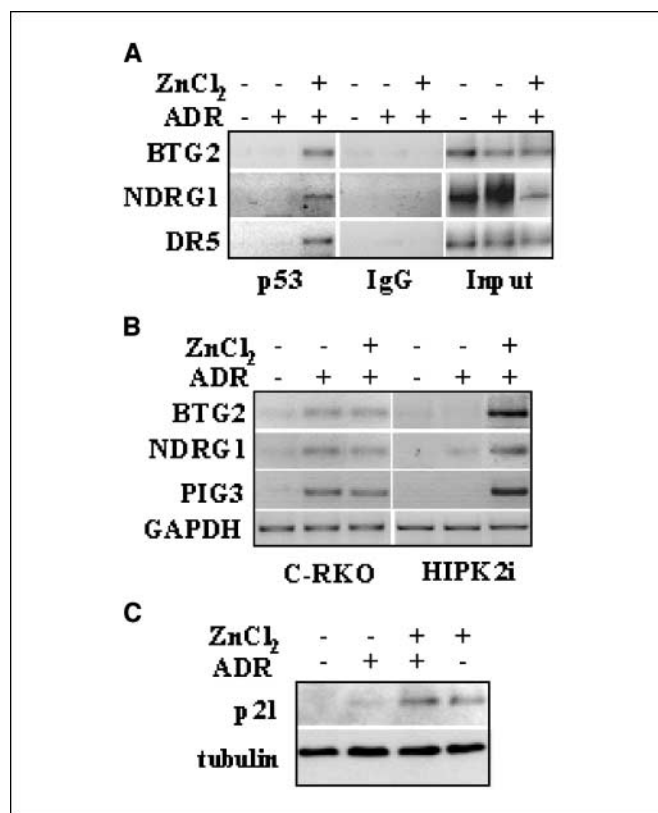


Figure 5. Reactivation of dysfunctional p53 in HIPK2i cells following zinc supplementation. *A*, ChIP analyses performed with p53 antibody on HIPK2i cells treated with ZnCl₂ and Adriamycin for 16 h. Nonspecific IgG was used as control. PCR analysis showed increased p53 binding to the selected target gene promoters in response to Adriamycin only after zinc supplementation. *B*, RT-PCR analyses of the indicated p53 target genes in C-RKO and HIPK2i cells treated with ZnCl₂ and Adriamycin. PCR showed regaining of wtp53-dependent gene expression in HIPK2i cells only after zinc supplementation to Adriamycin treatment. The mRNA levels were normalized to GAPDH expression. *C*, accumulation of p21 in HIPK2i cells treated as in *B*, as measured by immunoblotting. Anti-tubulin is used as protein loading control.

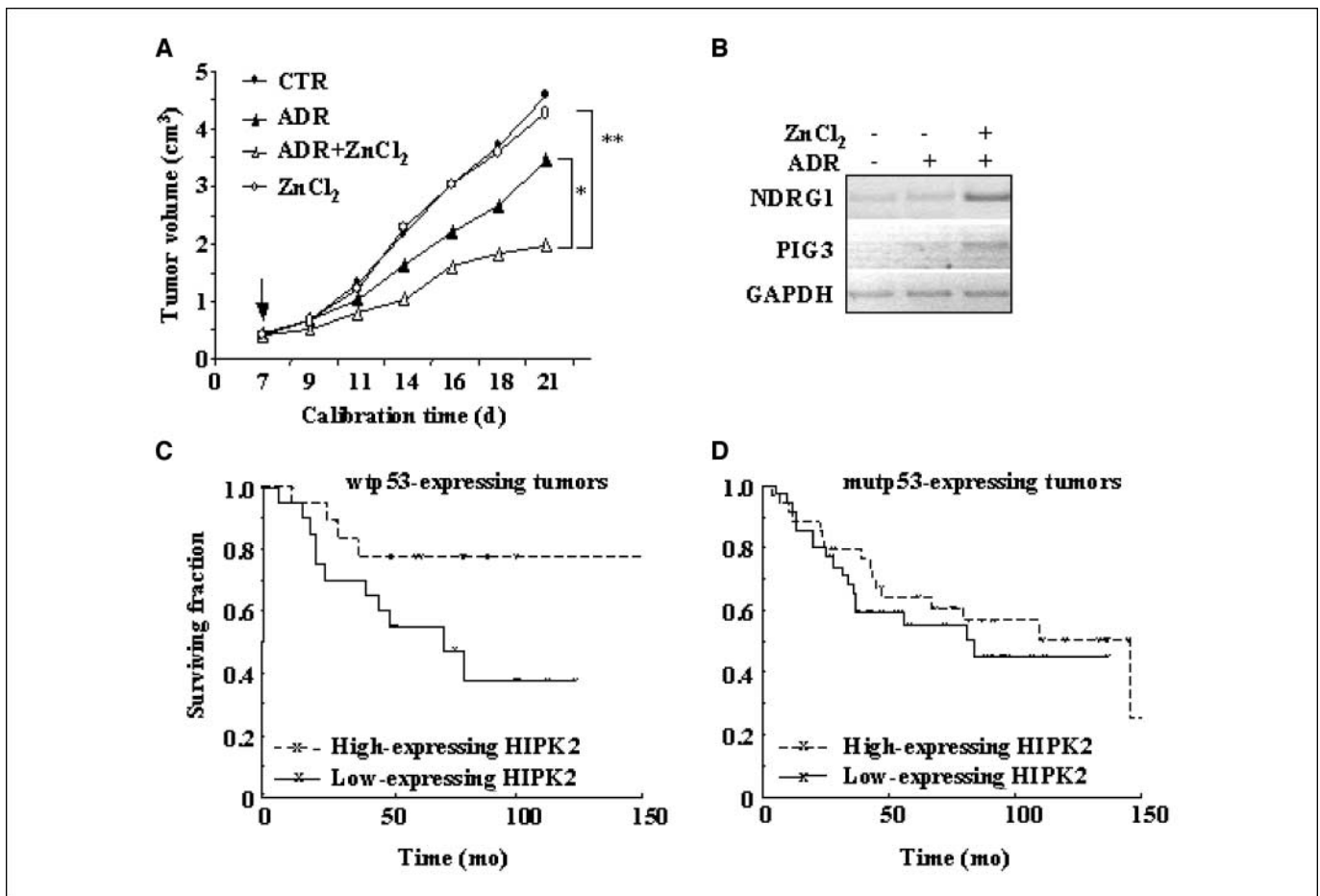


Figure 6. Growth inhibition of HIPK2i-derived tumors by combination treatment with ZnCl₂ and Adriamycin. **A**, tumor volumes were measured every other day following the establishment of xenografts in nude mice. HIPK2i-derived tumors were treated with Adriamycin at day 7 (arrow) and daily, starting from day 7, with ZnCl₂ administered for 2 wk. Y axis, tumor volume; X axis, calibration time after cell injection. The results showed a statistically significant reduction of tumor growth with combination treatment of zinc plus Adriamycin. *P* values of <0.05 (*) and <0.001 (**) were deemed statistically significant. **B**, RT-PCR analyses of HIPK2i-derived tumors as in **A** performed at day 18 showed regaining of p53 transcription activity of p53 target genes only after zinc supplementation to Adriamycin treatment. The mRNA levels were normalized to GAPDH expression. **C** and **D**, Kaplan-Meier plot comparing survival of colon cancer patients with high (top tertile) and low (bottom tertile) expression levels of the *HIPK2* gene. Kaplan-Meier analysis was performed separately on patients with wtp53 (*n* = 20 in each group; **C**) and mutp53 (*n* = 35 in each group; **D**). The x marks denote censored patients. Colon cancer patients with low *HIPK2* expression levels show poor, significantly (*P* = 0.05) lower survival rates in the wtp53 group; in the mutp53, *HIPK2* expression has no significant association with outcome (*P* = 0.45).

showed a significant association between low expression of *HIPK2* and poor outcome for patients with wtp53 tumors but not with mutp53. The presence of dysfunctional wtp53 in tumors correlates also with recent results that show growth-promoting activity by p73, another tumor suppressor of the p53 family (34). It also correlates with the finding that human p53 in the p53-null background of mice did not prevent accelerated tumor development after genotoxic or oncogenic stress (35). These findings imply that wtp53 can lose its oncosuppressor activity depending on interaction with other proteins. It also may correlate with the recent unexpected clinical analysis of ovarian cancer where cancer patients with wtp53 display a reduced long-term survival compared with those with mutp53 (36). The possibility that wtp53 *in vivo* may fluctuate between growth promoter and growth suppressor was suggested in the past as the conformational hypothesis for p53 function (37). Our study is limited thus far to the situation of wtp53 in tumor cells that lack *HIPK2*.

In conclusion, our results may open new ways to affect the possible equilibrium between active and inactive wtp53 in tumors toward increasing wtp53 oncosuppressor function, which may be applied in the clinic. They directly raise the possibility that

combination of chemotherapy and zinc may facilitate enhanced tumor growth inhibition, particularly in cancers with known wtp53 and low expression of *HIPK2*.

Disclosure of Potential Conflicts of Interest

No potential conflicts of interest were disclosed.

Acknowledgments

Received 12/21/2007; revised 2/22/2008; accepted 3/1/2008.

Grant support: Associazione Italiana per la Ricerca sul Cancro (AIRC) and Miur-Cofin (G. D'Orazi), EU Active p53 Consortium and AIRC-ROC (G. Blandino), Wolfson Family Charitable Trust on Tumour Cell Diversity (D. Givol and E. Domany), Ridgefield Foundation, EU MutP53 Consortium (E. Domany), and Kahn Family Foundation (G. Rechavi), E. Domany and D.A. Notterman are Principal Investigators of a National Cancer Institute Program Project Grant (P01-CA65930).

The costs of publication of this article were defrayed in part by the payment of page charges. This article must therefore be hereby marked *advertisement* in accordance with 18 U.S.C. Section 1734 solely to indicate this fact.

We thank G. Bossi and A. Gurtner for helpful advice and stimulating discussion; M. Onisto, D. Guidolin, and A.S. Belloni for immunohistochemical evaluation; S. Soddu for critical reading of the manuscript; and F. Barany (Weill Medical College, Cornell University, New York, NY) and P.B. Paty (Memorial Sloan-Kettering Cancer Center, New York, NY) for the colon cancer microarray data.

References

1. Hollstein M, Hergenhahn M, Yang Q, Bartsch H, Wang ZQ, Hainaut P. New approaches to understanding p53 gene tumor mutation spectra. *Mutat Res* 1999;432:199–209.
2. Vousden KH, Prives C. P53 and prognosis: new insights and further complexity. *Cell* 2005;120:7–10.
3. Brooks CL, Gu W. Ubiquitination, phosphorylation and acetylation: the molecular basis for p53 regulation. *Curr Opin Cell Biol* 2003;2:164–71.
4. Kannan K, Amariglio N, Rechavi G, et al. DNA microarrays identification of primary and secondary target genes regulated by p53. *Oncogene* 2001;20:2225–34.
5. Oda K, Arakawa H, Tanaka T, et al. P53AIP1, a potential mediator of p53-dependent apoptosis, and its regulation by Ser-46-phosphorylated p53. *Cell* 2000;102:849–62.
6. Mayo LD, Rok Seo Y, Jackson MW, et al. Phosphorylation of human p53 at serine 46 determines promoter selection and whether apoptosis is attenuated or amplified. *J Biol Chem* 2005;280:25953–9.
7. Di Lello P, Miller Jenkins LM, Jones TN, et al. Structure of the Tfb1/p53 complex: insights into the interaction between the p62/Tfb1 subunit of TFIIF and the activation domain of p53. *Mol Cell* 2006;22:731–40.
8. D'Orazi G, Cecchinelli B, Bruno T, et al. Homeodomain-interacting protein kinase-2 phosphorylates p53 at Ser46 and mediates apoptosis. *Nat Cell Biol* 2002;4:11–9.
9. Hofmann TG, Moller A, Sirma H, et al. Regulation of p53 activity by its interaction with homeodomain-interacting protein kinase-2. *Nat Cell Biol* 2002;4:1–10.
10. Di Stefano V, Rinaldo C, Sacchi A, Soddu S, D'Orazi G. Homeodomain-interacting protein kinase-2 activity and p53 phosphorylation are critical events for cisplatin-mediated apoptosis. *Exp Cell Res* 2004;293:311–20.
11. Pistritto G, Puca R, Nardinocchi L, Sacchi A, D'Orazi G. HIPK2-induced p53Ser46 phosphorylation activates the KILLER/DR5-mediated caspase-8-extrinsic apoptotic pathway. *Cell Death Differ* 2007;14:1837–9.
12. Li X-L, Harada H, Shima Y, et al. Mutations of the HIPK2 gene in acute myeloid leukemia and myelodysplastic syndrome impair AML1- and p53-mediated transcription. *Oncogene* 2007;26:7231–9.
13. Cho YJ, Gorina PD, Jeffrey A, Pavletich NP. Crystal structure of a p53 tumor suppressor DNA complex: understanding tumorigenic mutations. *Science* 1994;265:346–55.
14. Hainaut P, Milner J. A structural role for metal ions in the "wild-type" conformation of the tumor suppressor protein p53. *Cancer Res* 1993;53:1739–42.
15. Verhaegh GW, Parat MO, Richard MJ, Hainaut P. Modulation of p53 conformation and DNA-binding activity by intracellular chelation of zinc. *Mol Carcinog* 1998;21:205–14.
16. Meplan C, Richard M-J, Hainaut P. Metalloregulation of the tumor suppressor protein p53: zinc mediates the renaturation of p53 after exposure to metal chelators *in vitro* and in intact cells. *Oncogene* 2000;19:5227–36.
17. Tsafirir I, Tsafirir D, Ein-Dor L, Zuk O, Notterman DA, Domany E. Sorting points into neighborhoods (SPIN): data analysis and visualization by ordering distance matrices. *Bioinformatics* 2005;21:2301–8.
18. Di Stefano V, Soddu S, Sacchi A, D'Orazi G. HIPK2 contributes to PCAF-mediated p53 acetylation and selective transactivation of p21Waf1 after non-apoptotic DNA damage. *Oncogene* 2005;24:5431–42.
19. D'Orazi G, Sciuilli MG, Di Stefano V, et al. Homeodomain-interacting protein kinase-2 restrains cytosolic phospholipase A2-dependent prostaglandin E2 generation in human colorectal cancer cells. *Clin Cancer Res* 2006;12:735–41.
20. Wei C-L, Wu Q, Vega VB, et al. A global map of p53 transcription-factor binding sites in the human genome. *Cell* 2006;124:207–19.
21. Weisz L, Oren M, Rotter V. Transcription regulation by mutant p53. *Oncogene* 2007;26:2202–11.
22. Gannon JV, Greaves R, Iggo R, Lane DP. Activating mutations in p53 produce a common conformational effect. A monoclonal antibody specific for the mutant form. *EMBO J* 1990;9:1595–602.
23. Legros Y, Meyer A, Oryt K, Soussi T. Mutations in p53 produce a common conformational effect that can be detected with a panel of monoclonal antibodies directed toward the central part of the p53 protein. *Oncogene* 1994;9:3689–94.
24. Tsafirir D, Bacolod M, Selvanayagam Z, et al. Relationship of gene expression and chromosomal abnormalities in colorectal cancer. *Cancer Res* 2006;66:2129–37.
25. Vousden KH, Lane DP. p53 in health and disease. *Nat Rev Mol Cell Biol* 2007;8:275–83.
26. Lee H, Mok KH, Muhandiram R, et al. Local structural elements in the mostly unstructured transcriptional activation domain of human p53. *J Biol Chem* 2000;275:29426–32.
27. Haynes C, Oldfield CJ, Ji F, et al. Intrinsic disorder is a common feature of hub proteins from four eukaryotic interactomes. *PLoS Comput Biol* 2006;2:e100.
28. Friedlander P, Legros Y, Soussi T, Prives C. Regulation of mutant p53 temperature-sensitive DNA binding. *J Biol Chem* 1996;271:25468–78.
29. Joenger AC, Fersht AR. Structure-function-rescue: the diverse nature of common p53 cancer mutants. *Oncogene* 2007;26:2226–42.
30. Coyle P, Philcox JC, Carey LC, Rofe AM. Metallothionein: the multipurpose protein. *Cell Mol Life Sci* 2002;59:627–47.
31. Butler JS, Loh SN. Zn²⁺-dependent misfolding of the p53 DNA binding domain. *Biochemistry* 2007;46:2630–9.
32. Cherian MG, Jayasurya A, Bay B-H. Metallothioneins in human tumors and potential roles in carcinogenesis. *Mutat Res* 2003;533:201–9.
33. Calzado MA, Renner F, Roscic A, Schmitz ML. HIPK2: a versatile switchboard regulating the transcription machinery and cell death. *Cell Cycle* 2007;6:139–43.
34. Vikhansaya F, Toh WH, Dulloo I, et al. P73 supports cellular growth through c-Jun-dependent Ap-1 transactivation. *Nat Cell Biol* 2007;9:698–705.
35. Dudgeon C, Kek C, Demidov ON, et al. Tumor susceptibility and apoptosis defect in a mouse strain expressing a human p53 transgene. *Cancer Res* 2006;66:2928–36.
36. Moreno CS, Matyunina L, Dickerson EB, et al. Evidence that p53-mediated cell-cycle-arrest inhibits chemotherapeutic treatment of ovarian carcinomas. *PLoS ONE* 2007;5:e441.
37. Milner J. A conformation hypothesis for the suppressor and promoter functions of p53 in cell growth control and in cancer. *Proc Biol Sci* 1991;245:139–45.

Cancer Research

The Journal of Cancer Research (1916–1930) | The American Journal of Cancer (1931–1940)

Reversible Dysfunction of Wild-Type p53 following Homeodomain-Interacting Protein Kinase-2 Knockdown

Rosa Puca, Lavinia Nardinocchi, Hilah Gal, et al.

Cancer Res 2008;68:3707-3714.

Updated version Access the most recent version of this article at:
<http://cancerres.aacrjournals.org/content/68/10/3707>

Supplementary Material Access the most recent supplemental material at:
<http://cancerres.aacrjournals.org/content/suppl/2008/05/14/68.10.3707.DC1>

Cited articles This article cites 37 articles, 9 of which you can access for free at:
<http://cancerres.aacrjournals.org/content/68/10/3707.full#ref-list-1>

Citing articles This article has been cited by 3 HighWire-hosted articles. Access the articles at:
<http://cancerres.aacrjournals.org/content/68/10/3707.full#related-urls>

E-mail alerts [Sign up to receive free email-alerts](#) related to this article or journal.

Reprints and Subscriptions To order reprints of this article or to subscribe to the journal, contact the AACR Publications Department at pubs@aacr.org.

Permissions To request permission to re-use all or part of this article, use this link
<http://cancerres.aacrjournals.org/content/68/10/3707>.
Click on "Request Permissions" which will take you to the Copyright Clearance Center's (CCC) Rightslink site.